

Possible Young Stellar Objects without Detectable CO Emission

Ikuru IWATA,^{1,3} Shin-ichiro OKUMURA,² and Mamoru SAITO³

¹ Toyama Astronomical Observatory, Toyama Science Museum, 49-4 San-no-kuma, Toyama, Toyama 930-0155

² Okayama Astrophysical Observatory, National Astronomical Observatory, Kamogata-cho, Okayama 719-0232

³ Department of Astronomy, Faculty of Science, Kyoto University, Sakyo-ku, Kyoto 606-8502

E-mail (II): iwata@kusastro.kyoto-u.ac.jp

(Received 1997 November 13; accepted 1999 August 2)

Abstract

Young stellar objects (YSOs) usually appear in molecular clouds as infrared objects associated with a molecular envelope. Wouterloot and Brand (1989, AAA 50.133.012) searched 1302 IRAS point sources with reliable fluxes at 25, 60, and 100 μm near to the galactic plane for $^{12}\text{CO}(J = 1 - 0)$ emission; 1077 sources were detected. Among their far-infrared sources without detectable CO emission, we found that at least 18 objects are invisible at optical and near-infrared wavelengths. The infrared spectral indices between 2.2 μm and 25 μm correspond to those of class I YSOs, and the IRAS colors are similar to those of the usual YSOs. These peculiar far-infrared objects are highly concentrated around the galactic plane and the distances are estimated to be ~ 1 kpc. Although their distribution is away from molecular clouds, some of them seem to be associated with large dark clouds or weak radio sources. These objects are possible YSOs with low CO abundance in the envelopes.

Key words: Stars: formation — Infrared: stars — Circumstellar matter — Young stellar objects: search

1. Introduction

Most of stars burstly form in molecular clouds. Low-mass stars are also born in globules that are dispersely distributed in spiral arms (e.g., Yun, Clemens 1994). Based on the spatial distribution, age distribution, and kinematics of T Tauri stars, Feigelson (1996) claims that dispersed T Tauri stars with various ages consist of components drifting outward from currently active sites of star formation in molecular clouds, and components formed in now-dissipated clouddlets in past molecular cloud complexes (see Neuhauser 1997).

Young stellar objects (YSOs) grow in molecular cores up to the maximum luminosity phase while showing spectral energy distributions (SEDs) with a peak at the far-infrared (FIR) wavelength. The gas-to-dust mass ratio in molecular cores is considered to be similar to the interstellar value, because the core masses derived from the intensities of dust emission (e.g., Walker et al. 1990) are consistent with those derived from CO lines or other molecular lines (e.g., Casoli et al. 1986; Benson, Myers 1989; Wouterloot et al. 1989). In low-mass pre-main sequence stars, such as T Tauri stars, however, the envelope masses derived from the intensities of dust emission are larger than those derived from the CO line intensities (e.g., Dutrey et al. 1996); it has occurred at some stage from YSOs to pre-main sequence stage that

CO molecules have been removed from the envelopes or locked up on grains or more complex molecules in the envelopes (e.g., Aikawa et al. 1997).

In this paper, we show the presence of 18 bright FIR objects peculiar in the sense that they are not detectable in the ^{12}CO line, show the class I YSOs' SEDs and are located away from molecular clouds. Section 2 describes the sample. In section 3 we consider infrared SED indices of the sample using data of IRAS and our near-infrared photometry, and show that the indices correspond to those of class I YSOs. In section 4 we discuss the IRAS colors, sky distribution, and luminosities of the sample. In section 5 we give a summary.

2. Sample

Wouterloot and Brand (1989) made a complete search for the $^{12}\text{CO}(J = 1 - 0)$ line on 1302 IRAS point sources with reliable flux densities at 25, 60, and 100 μm (Joint IRAS Science Working Group 1988; IRAS PSC) and with characteristic FIR colors of YSOs in a zone of $\ell = 85^\circ$ to 280° and $b = -10^\circ$ to 10° (we hereafter call those WB objects); their beam size and rms noise level were 43'' and 0.2–1.0 K for SEST observations, and 21'' and 0.7–1.5 K for IRAM observations, respectively. The velocity ranges of their ^{12}CO observations are 220 km s^{-1} with a central

velocity of 60 km s^{-1} for SEST observations, and 208 km s^{-1} with central velocities of -50 to 20 km s^{-1} for IRAM observations. They detected CO emission on 1077 point sources (82.7%), and no emission on another 223 sources. Wouterloot et al. (1990) considered that WB objects without detectable CO emission are extragalactic objects because of the homogeneous sky distribution in the surveyed region, in contrast with the distribution of WB objects with CO emission concentrated around the galactic plane. We examined the literature and optical images on Schmidt plates for all 223 WB objects without CO emission, and found that 132 are associated with optical objects, which are early-type stars, planetary nebulae, and galaxies. But the remaining 91 WB objects do not have any distinct optical counterparts at the positions of the IRAS point sources. The results are summarized in table 1.

Iwata et al. (1997) carried out near-infrared imaging observations of 55 objects among the 91 optically invisible WB objects without ^{12}CO emission at the Okayama Astrophysical Observatory (OAO). As a result, 16 objects were found to be galaxies and possible galaxies, 4 objects are H II regions and a possible H II region, and 14 objects are stars, while 21 objects don't show any counterparts, even in the J , H , and K' bands. The 21 WB objects invisible at optical and near-infrared wavelengths and not detectable in $^{12}\text{CO}(J=1-0)$ line were the sample of this study. We call those "peculiar FIR" objects. Iwata et al. (1997) claimed that these objects are mostly galactic objects because of the sky distribution along the galactic plane and the FIR colors colder than those of IRAS galaxies.

Figure 1 shows a relation of the $60 \mu\text{m}$ flux density in IRAS PSC versus the $^{12}\text{CO}(J=1-0)$ line intensity for 21 peculiar FIR objects and 97 WB objects with ^{12}CO emission existing at $\ell = 85^\circ$ to 105° . The CO intensities are the values of Wouterloot and Brand (1989); the single-line objects are preferentially adopted. For objects associated with multi-component CO lines we adopted a line if it is several times or more stronger than other components or it has some active features. For the peculiar FIR objects the upper limits are shown. We used the 97 WB objects shown by dots in figure 1 as a control sample, which are representatives of YSOs at around the maximum luminosity phase in molecular cores (Wouterloot et al. 1990). A correlation similar to that of the control sample is shown in Casoli et al. (1986). Figure 1 indicates that the peculiar FIR objects have relatively less strong $60 \mu\text{m}$ flux densities and extremely weak CO intensities among WB objects.

To ascertain the reality of the peculiar FIR objects, we requested the Infrared Processing Analysis Center (IPAC) for co-addition of the IRAS data. As results of the ADDSCAN-SCANPI programs, in which 6 to 21 scan data were coadded for each band of each object,

more reliable flux densities were obtained for the four bands of all objects, except for a $12 \mu\text{m}$ flux density of IRAS 22044+5451 and an $100 \mu\text{m}$ flux density of IRAS 04375+5016.

Table 2 lists 21 peculiar FIR objects with respect to the number of Wouterloot and Brand (1989), IRAS name, galactic coordinate transformed from the equatorial coordinate of IRAS point source, flux densities at 12 , 25 , 60 , and $100 \mu\text{m}$ quoted from IRAS PSC at the first line of each object and those of co-added data at the second line, three infrared colors calculated using the co-added data, infrared luminosity at 1 kpc (an assumed distance, described in subsection 4.2), and mode of our near-infrared observation. We computed the luminosity L_{IR} using an equation (Emerson 1988),

$$L_{\text{IR}} = 0.31d^2(20.653f_{12} + 7.538f_{25} + 4.578f_{60} + 1.762f_{100})L_{\odot}, \quad (1)$$

where f_{λ} is the co-added flux density in Jy and d is a distance in kpc.

3. Observations and Results

The near-infrared imaging observations were carried out at OAO on 1995 August and 1996 February using Okayama Astrophysical System for Infrared imaging and Spectroscopy (OASIS) with a detector NICMOS-3 equipped on the 1.88 m reflector (Yamashita et al. 1995). The FOV was $4' \times 4'$ and the pixel size was $0.^{\prime\prime}97$. The exposure times were 300 s, 150 s, and 225 s at the J , H , and K' bands, respectively, for 18 objects, and 600 s at J or H bands for the other three objects (see table 2). The details of the observations and data reduction were shown in Iwata et al. (1997). Figure 2 shows the optical and near-infrared images of $1.^{\prime}2 \times 1.^{\prime}2$ around the 21 objects. The optical images were made from Digitized Sky Surveys produced at the Space Telescope Science Institute based on photographic data obtained using the Oschin Schmidt Telescope on Palomar Mountain. At the positions of IRAS point sources which are indicated by the position uncertainty ellipses quoted in IRAS PSC, we could not find any distinct optical or near-infrared counterpart.

During the observations we observed three photometric standard stars, HD 44612, BD $+0^\circ 1694$, and HD 105601 (Elias et al. 1982); their K magnitudes are 7.040, 4.585, and 6.685, respectively. For a detection limit of $S/N=10$, we obtained the limiting magnitudes to be $K' = 14.3$ to 15.2 for 225 s exposure, where the range of magnitudes was due to the different sky conditions. The magnitude difference of the OASIS K' band ($2.16 \mu\text{m}$) and K band ($2.19 \mu\text{m}$) is less than 0.03 mag in the rms value for more than 50 stars (Okumura et al. 1999, in preparation). For a similar photometric system, Wainscoat and Cowie

(1992) derived $K' - K = 0$ to 0.08 mag for 18 stars. We assume the OASIS K' magnitude to be equivalent to the K magnitude. The 18 peculiar FIR objects from WB 70 to WB 584 listed in table 2 are less bright than $K = 14.3$. We thus adopt $K = 13.7$ as the upper limit for the 18 peculiar FIR objects, assuming an interstellar extinction less than $0.^m6$ at the K band, i.e., $A_V < 5.6$ (Mathis 1990).

The K magnitude is transformed to flux density f_K in Jy, following Bessell and Brett (1988); i.e.,

$$\log f_K = 0.4(13 - K) - 2.38. \quad (2)$$

Equation (2) yields $\log f_K = -2.66$ and $\log(\nu f)_K = 11.47$ for $K = 13.7$. The upper limit of $\log(\nu f)_K = 11.47$ is less than $\log(\nu f)_{25}$ at $25 \mu\text{m}$ for all of the 18 peculiar FIR objects, which are $\log(\nu f)_{25} = 13.08 + \log(f_{25}) > 12.3$ for their values of $f_{25} > 0.2 \text{ Jy}$, as shown in table 2. YSOs are classified by the spectral index, $\alpha = -d \log(\nu f_\nu) / d \log \nu$, between $2.2 \mu\text{m}$ and $25 \mu\text{m}$. Lada (1987) defined class I YSOs to be objects with $\alpha_{2.2, 25} > 0$, and class II YSOs to be $-2 < \alpha_{2.2, 25} < 0$. Class I YSOs are usually invisible at optical wavelengths because of heavy obscuration by dense molecular clouds, and they are considered to be at an early stage of stellar evolution. Typical class II YSOs are T Tauri stars. All of the 18 peculiar FIR objects have positive α -indices corresponding to class I YSOs. For the remaining three objects (WB 628, WB 901, and WB 1001), we can not give $\alpha_{2.2, 25}$. Although the exposure times at the J and H bands for these objects were longer than those for the other 18 objects, we found no counterpart within the position uncertainty ellipses of the IRAS point sources. In the following discussion we include these objects in the peculiar FIR objects.

The α -indices of all of the peculiar FIR objects are also positive between $\lambda = 25 \mu\text{m}$ and $60 \mu\text{m}$, where $\alpha_{25, 60} = 2.63 \log(f_{60}/f_{25}) - 1$ (see table 2). But the values of $\alpha_{12, 25} = 3.137 \log(f_{25}/f_{12}) - 1$ are negative for 12 peculiar FIR objects with $\log(f_{25}/f_{12}) < 0.32$ (see table 2). This means that more than half of the peculiar FIR objects have a second peak at between $2.2 \mu\text{m}$ and $25 \mu\text{m}$.

4. Discussion

4.1. Features of the Peculiar FIR Objects

Figures 3 and 4 show IRAS color-color diagrams for the peculiar FIR objects, the control sample, which are usual YSOs, and cirrus. The cirrus colors indicated by the open circles were measured by Boulanger and Perault (1988) in 8 nearby molecular clouds, and the filled circle stands for the FIR color of warm cirrus in the H I cloud at high galactic latitude (Boulanger et al. 1985). Clemens et al. (1991) measured the infrared colors of 248 globules and small molecular clouds, and obtained the mean

values and dispersions to be $\log(f_{100}/f_{60}) = 0.70 \pm 0.20$, $\log(f_{60}/f_{25}) = 0.68 \pm 0.34$, and $\log(f_{25}/f_{12}) = 0.01 \pm 0.30$; these are similar to the colors of cirrus described in Boulanger and Perault (1988). Clemens et al. interpreted the infrared emission of globules to be cirrus. We find in figures 3 and 4 that the IRAS colors of the peculiar FIR objects resemble those of the usual YSOs rather than the colors of cirrus, except for the warm cirrus.

Among the visually known WB objects without a detectable ^{12}CO line, there are early-type stars, and their number is as many as about half of the galaxies, as shown in table 1. In table 3, such 11 early-type stars with reliable $12 \mu\text{m}$ flux densities are given. The seven stars from B5 to A2 are possibly associated with IRAS point sources having $f_{60} \simeq 2 \text{ Jy}$ to 12 Jy , which are similar values to those of the peculiar FIR objects. The visual magnitudes are 5 to 9 mag, and thus the K magnitudes are brighter than 9 mag (Bessell, Brett 1988). In order to make apparent K magnitudes of these stars be less than 13 mag due to extinction, the extinction value should be greater than $A_V \simeq 37$ (Mathis 1990), which is unusually large interstellar extinction. The latitude distributions differ between these stars and the peculiar FIR objects. The three B0 or OB stars listed in table 3 are also associated with IRAS point sources with $f_{60} \simeq 36 \text{ Jy}$ to 56 Jy ; the values are one order of magnitude larger than the typical values of the peculiar FIR objects. Putting these stars at distances three-times further than the present distances, we may obtain $m_V \simeq 11.5$ to 13 and $K > 12$. If there is an additional interstellar extinction of $A_V > 7^m$, we may find no object on these positions at visual and K bands for detection limits of $m_V = 19$ and $K = 13$. Such large interstellar extinctions are only caused by the presence of molecular clouds in the line of sight. But the peculiar FIR objects do not have detectable CO emission. We rule out the possibility that the peculiar FIR objects mostly correspond to obscured early-type stars with an FIR emitting envelope.

Galaxies have IRAS colors similar to those of YSOs in a range of $\log(f_{60}/f_{25}) = 0.6 - 1.2$ and $\log(f_{100}/f_{60}) = 0.0 - 0.6$ (e.g., Sauvage, Thuan 1994). It is still possible that a few of the peculiar FIR objects are obscured galaxies with intrinsically low surface brightness.

4.2. Distances and Luminosities of the Peculiar FIR Objects

About half of the 21 peculiar FIR objects are located within $b = 2^\circ$ and 90% are within 4° (see table 2). This concentration toward the galactic plane is higher compared with that of globules by Clemens and Barvainis (1988), who found the extent of the globules in b to be 10° to 12° . This suggests that the distances to the peculiar FIR objects are further than the typical distances of dark globules, $\sim 600 \text{ pc}$ (Clemens, Barvainis 1988). If

we take $\pm 4^\circ$ as the extent in b of the peculiar FIR objects and 87 pc as the layer thickness, the same as that of molecular gas within 1 kpc by Dame et al. (1987), the typical distances of the peculiar FIR objects are ~ 1.2 kpc. Note that the angular scale height of the ultra-compact H II regions is 0.6° , which corresponds to ~ 90 pc at the distance of the galactic center (Wood, Churchwell 1989).

For an assumed distance of 1 kpc, the peculiar FIR objects have luminosities of $\sim 4 L_\odot$ to $96 L_\odot$ (see table 2), which correspond to the highest values of YSOs in the Taurus–Auriga and Ophiucus regions (Kenyon et al. 1990). The peculiar FIR objects should have internal energy sources, and they seem to have intermediate YSO luminosities.

The beam size, $21''$, of Wouterloot and Brand's (1989) observations at IRAM for the 19 objects, except for WB 901 and WB 1001, corresponds to about $0.1d$ pc, where d is an assumed distance in kpc, and is comparable to or smaller than the typical CO core sizes at distances of $d < 3$ kpc. Thus, the weak CO intensities of the peculiar FIR objects are not caused by dilution effects.

4.3. Location of the Peculiar FIR Objects

The cirrus 2 flags (CIRR2) in IRAS PSC indicate a ratio of the cirrus flux, F_C to source flux at $100 \mu\text{m}$, F_S :

$$CIRR2 = (8/3) \log(F_C/F_S) + (19/3). \quad (3)$$

The distributions of the cirrus 2 flags are shown in table 4 for the control sample and the peculiar FIR objects; the peculiar FIR objects have flags by two grades higher than the control sample. The difference almost corresponds to the different $100 \mu\text{m}$ intensities between the peculiar FIR objects and the control sample (see figures 1 and 3); the cirrus intensities are not stronger around the peculiar FIR objects compared with the locations of the control sample.

YSOs leave its parent molecular cores with time, and the offset distances may become up to 1 pc for bright YSOs (e.g., Kenyon et al. 1990; Clark 1991). The peculiar FIR objects may have its parent molecular cores in the neighborhood. Dobashi et al. (1994) made a $^{13}\text{CO}(J=1-0)$ survey at a region of $\ell = 80^\circ$ to 104° and $b = -7.5^\circ$ to 10.5° with $2.7'$ angular resolution and $8'$ grid spacing; they detected emission lines $> 1.2 \text{ K km s}^{-1}$ at 2191 positions, or 9% of the observed points. Yonekura et al. (1997) made a successive ^{13}CO survey in the region $\ell = 100^\circ$ to 130° and $b = -10.5^\circ$ to 20° with a same beam size and a same grid spacing as Dobashi et al. (1994). Although there are 15 peculiar FIR objects among the regions of these two surveys, none of them are associated with the molecular clouds. The peculiar FIR objects at other regions are also not located on any molecular clouds detected by Dame et al. (1987).

At $\ell < 140^\circ$, 7 of the 17 peculiar FIR objects are located on or near to large Lynds dark clouds; these are WB 92 vs. Lynds 1083, WB 151 and 153 vs. Lynds 1107, WB 274 vs. Lynds 1238, WB 302 vs. Lynds 1264, and WB 425 and 428 vs. Lynds 1373 (Lynds 1962). These imply that the peculiar FIR objects tend to be associated with large dark clouds, or to be located at distances further than the large dark clouds. Yun and Clemens (1995) found 22 YSOs with near-infrared counterparts in globules and classified them into 10 class I objects and 12 class II objects. Their class I YSOs have $K = 9.8$ to 13.9 and the luminosities at assumed distance of 600 pc are similar to those of the peculiar FIR objects. There is, however, an outstanding difference that Yun and Clemens' class I YSOs almost have CO outflows (Yun, Clemens 1994), in contrast with the weak CO emissions of the peculiar FIR objects.

Four peculiar FIR objects (WB 72, 92, 127, and 157) are located near to radio sources with $18 - 39 \text{ mJy}$ at $\lambda \simeq 6 \text{ cm}$ (Gregory et al. 1996); the separations between the FIR and radio sources are $38''$ to $108''$. None of the peculiar FIR objects are on the X-ray point sources detected by ROSAT (Voges et al. 1994).

5. Summary

We found the presence of unusual IRAS point sources in the sense that they are bright at 25 , 60 , and $100 \mu\text{m}$ but invisible at optical and near-infrared wavelengths as well as in the ^{12}CO line. At least 18 such objects have α -indices between 2.2 and $25 \mu\text{m}$, corresponding to class I YSOs. The IRAS colors are similar to those of the usual YSOs; in detail, about half of them have a second peak at between $2.2 \mu\text{m}$ and $25 \mu\text{m}$ and the largest $\log(f_{100}/f_{60})$ values of YSOs. Although the peculiar FIR objects avoid molecular clouds, seven objects are located near to large dark clouds, and four are near to radio sources. The distances are induced to be around 1 kpc, implying that they are mostly YSOs with intermediate luminosities and low CO abundance in the envelopes.

Further observations of these objects in molecular lines and millimeter continuum are needed to clarify their nature.

SCANPI processing for IRAS data used in this study was made at IPAC (Infrared Processing and Analysis Center), which is operated by the California Institute of Technology, Jet Propulsion Laboratory under contract to the National Aeronautics and Space Administration (NASA). The Digitized Sky Surveys were produced at the Space Telescope Science Institute under U.S. Government grant NAG W-2166. We thank an anonymous referee who gave us helpful comments.

References

Acker A., Ochsenbein F., Stenholm B., Tylenda R., Marcout J., Schohn C. 1992, *Strasbourg-ESO Catalogue of Galactic Planetary Nebulae* (ESO, München)

Aikawa Y., Umebayashi T., Nakano T., Miyama S.M. 1997, *ApJ* 486, L51

Benson P.J., Myers P.C. 1989, *ApJS* 71, 89

Bessell M.S., Brett J.M. 1988, *PASP* 100, 1134

Boulanger F., Baud B., van Albada G.D. 1985, *A&A* 144, L9

Boulanger F., Perault M., 1988, *ApJ* 330, 964

Casoli F., Dupraz C., Gerin M., Combes F., Boulanger F., 1986, *A&A* 169, 281

Clark F.O. 1991, *ApJS* 75, 611

Clemens D.P., Barvainis R. 1988, *ApJS* 68, 257

Clemens D.P., Yun J.L., Heyer M.H. 1991, *ApJS* 75, 877

Dame T.M., Ungerechts H., Cohen R.S., de Geus E.J., Grenier I.A., May J., Murphy D.C., Nyman L.-Å., Thaddeus P. 1987, *ApJ* 322, 706

Dobashi K., Bernard J.-P., Yonekura Y., Fukui Y. 1994, *ApJS* 95, 419

Dutrey A., Guilloteau S., Duvert G., Prato L., Simon M., Schuster K., Ménard F. 1996, *A&A* 309, 493

Elias J.H., Frogel J.A., Matthews K., Neugebauer G. 1982, *AJ* 87, 1029

Emerson J.P. 1988, in *Formation and Evolution of Low Mass Stars*, ed A.K. Dupree, M.T.V.T. Lago (Kluwer, Dordrecht) p193

Feigelson E.D. 1996, *ApJ* 468, 306

Gregory P.C., Scott W.K., Douglas K., Condon J.J. 1996, *ApJS* 103, 427

Iwata I., Nakanishi K., Takeuchi T., Saitō M., Yamashita T., Nishihara E., Okumura S. 1997, *PASJ* 49, 47

Joint IRAS Science Working Group 1988, *IRAS Point Source Catalog, version 2* (NASA, Washington D.C.) (IRAS PSC)

Kenyon S.J., Hartmann L.W., Strom K.M., Strom S.E., 1990, *AJ* 99, 869

Lada C.J. 1987, in *Star Forming Regions*, ed M. Peimbert, *J. Jugaku* (Reidel, Dordrecht) p1

Lynds B.T. 1962, *ApJS* 7, 1

Mathis J.S. 1990, *ARA&A* 28, 37

Mermilliod J.-C., Mermilliod M. 1994, *Catalogue of Mean UVB data on Stars* (Springer-Verlag, New York)

Nakanishi K., Takata T., Yamada T., Takeuchi T.T., Shiroya R., Miyazawa M., Watanabe S., Saitō M. 1997, *ApJS* 112, 245

Neuhäuser R. 1997, *Science* 276, 1363

Nilson P. 1973, *Uppsala General Catalogue of Galaxies* (Uppsala Offset Center, Uppsala)

Sauvage M., Thuan T.X. 1994, *ApJ* 429, 153

Smithsonian Astrophysical Observatory 1966, *Star Catalog (Smithsonian Institution, Washington D.C.) (SAO)*

Takata T., Yamada T., Saitō M., Chamaux P., Kazés I. 1994, *A&AS* 104, 529

Voges W., Gruber R., Haberl F., Kuerster M., Pietsch W., Zimmermann U. 1994, *ROSAT Source Catalog, Version 11-May-1995*

Wackering L.R. 1970, *Mem. RAS* 73, 153

Wainscoat R.J., Cowie L.L. 1992, *AJ* 103, 332

Walker C.K., Adams F.C., Lada C.J. 1990, *ApJ* 349, 515

Wood D.O.S., Churchwell E. 1989, *ApJ* 340, 265

Wouterloot J.G.A., Brand J. 1989, *A&AS* 80, 149

Wouterloot J.G.A., Brand J., Burton W.B., Kwee K.K. 1990, *A&A* 230, 21

Yamada T., Takata T., Djameluddin T., Tomita A., Aoki K., Takeda A., Saitō M. 1993, *ApJS* 89, 57

Yamashita T., Nishihara E., Okumura S., Mori A., Watanabe E. 1995, in *Scientific and Engineering Frontiers for 8–10 m Telescopes in the 21th Century*, ed M. Iye, T. Nishimura (University Academy Press, Tokyo) p285

Yonekura Y., Dobashi K., Mizuno A., Ogawa H., Fukui Y. 1997, *ApJS* 110, 21

Yun M.L., Clemens D.P. 1994, *ApJS* 92, 145

Yun M.L., Clemens D.P. 1995, *AJ* 109, 742

Table 1. Optical counterparts of IRAS point sources not associated with the ^{12}CO line in Wouterloot and Brand's (1989) search.

Optical object	Number	Reference
star	41	SAO Star Catalog (1966), Wackering (1970), Mermilliod, Mermilliod (1994)
galaxy*	79	Nilson (1973), Yamada et al. (1993), Takata et al. (1994), Nakanishi et al. (1997)
planetary nebula	12	Acker et al. (1992)
unknown	91	

* The number of galaxies with known redshifts is 65 among them.

Table 2. IRAS data of the point sources invisible at optical and near-infrared wavelengths and having no detectable ^{12}CO line.

WB No.	IRAS name	ℓ	b	f_{12} (Jy)	f_{25} (Jy)	f_{60} (Jy)	f_{100} (Jy)	f_{25}/f_{12}	logarithm of f_{60}/f_{25}	f_{100}/f_{60}	L_{IR}^* (L_\odot)	NIR obs. [†]
70	21188+5517	96.05	4.06	0.49	0.49	10.38	43.63	—	—	—	48	1
				0.55	0.55	10.44	52.16	0.0	1.28	0.70	—	—
72	21199+4949	92.32	0.06	0.25L	1.30	7.70	15.39	—	—	—	25	1
				0.07	1.52	8.79	15.41	1.34	0.76	0.24	—	—
92	21306+5532	97.45	3.09	0.73	1.91	24.86	65.19	—	—	—	—	—
				0.85	2.37	30.33	76.67	0.45	1.11	0.40	96	1
117	21422+5625	99.24	2.67	0.36	0.49	6.94	31.35	—	—	—	35	1
				0.51	0.59	6.63	38.02	0.06	1.05	0.76	—	—
119	21426+5723	99.92	3.38	0.25L	0.28	3.39	12.66	—	—	—	—	—
				0.27	0.37	3.50	12.47	0.14	0.98	0.55	14	1
127	21472+5642	99.95	2.44	0.25L	0.29	4.22	18.15	—	—	—	—	—
				0.22	0.39	5.22	15.73	0.25	1.13	0.48	18	1
151	22035+5442	100.56	-0.54	0.25L	0.30	3.90	8.13	—	—	—	—	—
				0.11	0.27	4.01	8.63	0.39	1.17	0.33	12	1
153	22044+5451	100.74	-0.49	0.25L	0.25	1.45	4.28	—	—	—	—	—
				—	0.26	1.49	6.97	—	0.76	0.67	7:	1
157	22096+5725	102.81	1.19	0.25L	0.40	7.70	25.57	—	—	—	—	—
				0.30	0.51	8.96	28.61	0.23	1.24	0.50	31	1
168	22169+5316	101.37	-2.83	0.25L	0.43	1.31	2.53	—	—	—	—	—
				0.06	0.27	1.34	2.87	0.65	0.70	0.33	4	1
246	23055+5913	110.10	-0.77	0.26L	0.40	6.87	27.07	—	—	—	—	—
				0.18	0.71	6.95	30.83	0.60	0.99	0.65	29	1
260	23122+5758	110.45	-2.25	0.34	0.96	6.86	11.94	—	—	—	—	—
				0.39	1.82	7.14	10.91	0.67	0.59	0.18	23	1
272	23190+5637	110.83	-3.84	0.25L	0.50	1.65	3.02	—	—	—	—	—
				0.11	0.54	1.86	3.34	0.69	0.54	0.25	6	1
274	23217+6028	112.45	-0.33	0.37L	0.53	4.26	14.79	—	—	—	—	—
				0.11	0.63	4.20	17.53	0.76	0.82	0.62	18	1
302	23504+6802	117.55	6.07	0.26	0.52	5.49	13.65	—	—	—	—	—
				0.32	0.58	5.42	12.45	0.26	0.97	0.36	18	1
425	02264+6034	134.70	0.20	0.44	0.63	12.96	50.79	—	—	—	—	—
				0.53	0.95	14.65	58.94	0.25	1.19	0.60	59	1
428	02309+6034	135.21	0.41	0.59	0.96	9.59	29.53	—	—	—	—	—
				0.70	1.18	11.32	35.91	0.23	0.98	0.50	43	1
584	04375+5016	155.50	2.65	0.31L	0.47	4.54	8.57	—	—	—	—	—
				0.37	0.47	4.53	—	0.10	0.98	—	10:	1
628	05183+3323	173.43	-1.86	0.66	1.02	14.70	44.07	—	—	—	—	—
				0.75	1.29	12.78	56.27	0.24	1.00	0.64	57	H
901	06486-0110	214.02	-0.61	0.48	0.54	5.88	23.50	—	—	—	—	—
				0.55	0.61	6.25	26.04	0.04	1.01	0.62	28	J
1001	07272-1909	234.31	-0.68	0.25L	0.28	2.31	8.87	—	—	—	—	—
				0.30	0.37	2.79	11.08	0.09	0.88	0.60	13	J

* For an assumed distance of 1 kpc.

† 1: the exposure time was 300 s at J -band, 150 s at H -band, and 225 s at K' -band. H: the exposure time was 600 s at H -band. J: the exposure time was 600 s at J -band.

Table 3. IRAS point sources without CO emission and associated with known stars.

WB No.	IRAS name	ℓ	b	f_{12} (Jy)	f_{25} (Jy)	f_{60} (Jy)	f_{100} (Jy)	Star SAO Sp m_v	Sep.*	Ref. [†]
17	20556+4806	88.34	1.80	0.35	0.91	9.75	27.05	050280 A0 8.4	6''	1
164	22150+6109	105.49	3.89	0.35	1.92	36.71	78.53	Em. star 11B	2''	2
167	22162+5539	102.60	-0.78	0.70	2.49	36.64	93.46	B0 10.4	15''	3
207	22444+5853	107.51	0.09	0.43	1.57	14.38	33.75	Em. star	35''	2
454	02495+6414	135.64	4.64	0.40	1.15	11.77	26.01	012493 B8 8.6	9''	1
575	04331+5211	153.62	3.40	0.23	0.46	2.95	7.62	024716 A0 8.7	22''	1
600	05017+2639	176.80	-8.71	0.43	0.69	2.48	6.59	076945 A2 7.7	7''	1
645	05247+3422	173.37	-0.20	1.66	5.03	56.89	135.78	058067 B0 9.1	64''	1
655	05293+1701	188.50	-8.89	0.43	1.23	3.74	4.06	094630 B9 6.0	4''	1
893	06467-1505	226.21	-7.38	0.43	1.62	4.60	5.68	151962 B5 5.3	15''	1
1177	08428-3657	258.27	3.52	0.26	0.88	5.05	9.21	199573 B8 5.8	64''	1

* The separations given in IRAS PSC.

† 1: Star Catalog (SAO 1966), 2: Wackering (1970), and 3: Mermilliod and Mermilliod (1994).

Table 4. Distribution of IRAS cirrus 2 flags for the control sample and the peculiar FIR objects.

Flag	1	2	3	4	5	6	7	8	9	total
Control sample	1	3	20	21	28	19	4	1	0	97
Peculiar objects	0	0	1	1	2	6	7	3	1	21

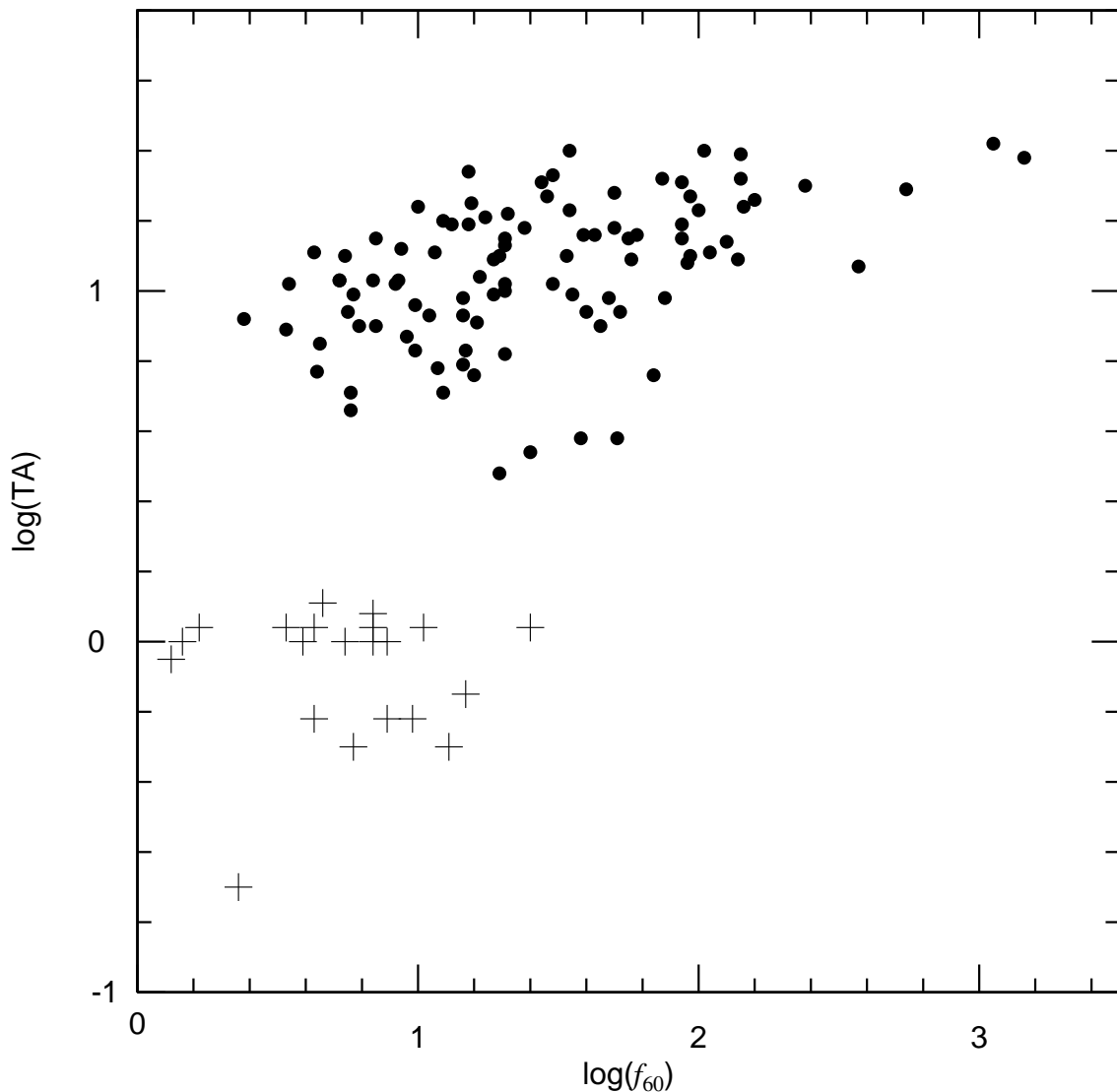


Fig. 1.. IRAS 60 μ m flux density (Jy) versus the $^{12}\text{CO}(J = 1 - 0)$ line intensity (K) for IRAS point sources obtained by Wouterloot and Brand (1989). The dots indicate 97 objects with ^{12}CO emission. The crosses indicate 21 objects, the CO intensities of which are the upper limits in the Wouterloot and Brand' observations. The 21 objects are also invisible in the optical and near-infrared wavelengths.

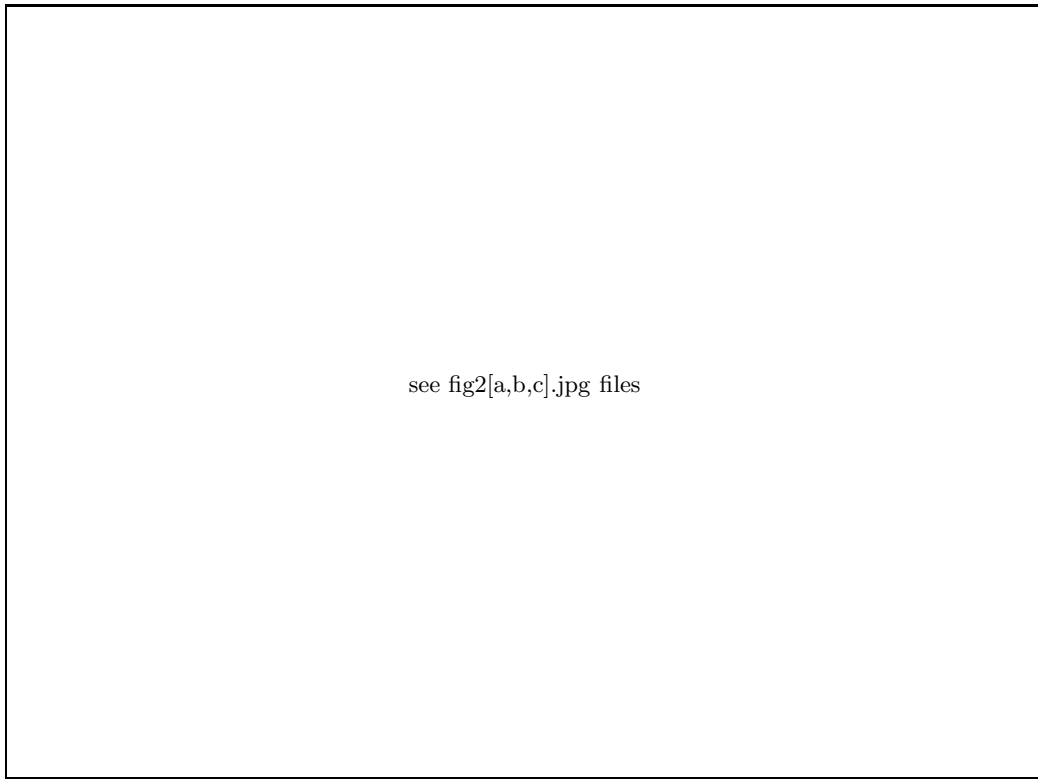


Fig. 2.. Sample images at optical and near-infrared wavelengths around peculiar FIR objects. The optical images were made from the Digitized Sky Survey and the near-infrared images were taken at OAO by using OASIS; the 18 near-infrared images, except for last three, are at the K' band, and for IRAS 05183+3323 it is at the H band, and for the last two at the J band. The FOV is $1.2' \times 1.2'$. The ellipses are the position uncertainty ellipses taken from IRAS PSC.

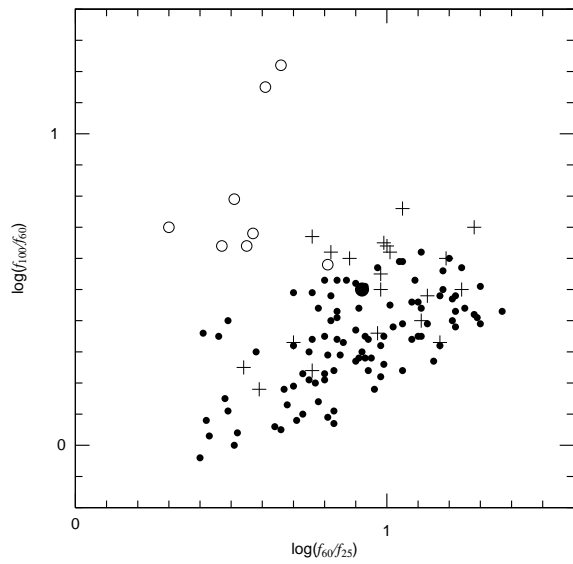


Fig. 3.. IRAS color-color diagram of the peculiar FIR objects (crosses), the control sample (dots), and cirrus (open and filled circles). f_λ is the IRAS flux density at $\lambda \mu\text{m}$.

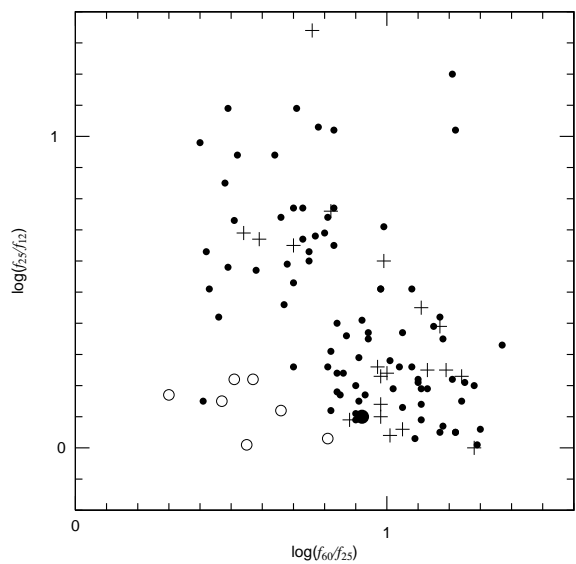


Fig. 4.. Same as figure 3, but for the colors of $\log(f_{60}/f_{25})$ versus $\log(f_{25}/f_{12})$.

This figure "fig2a.jpg" is available in "jpg" format from:

<http://arxiv.org/ps/astro-ph/9909387v1>

This figure "fig2b.jpg" is available in "jpg" format from:

<http://arxiv.org/ps/astro-ph/9909387v1>

This figure "fig2c.jpg" is available in "jpg" format from:

<http://arxiv.org/ps/astro-ph/9909387v1>